The Development of a Digital Design Workflow for the Surgical Obturator

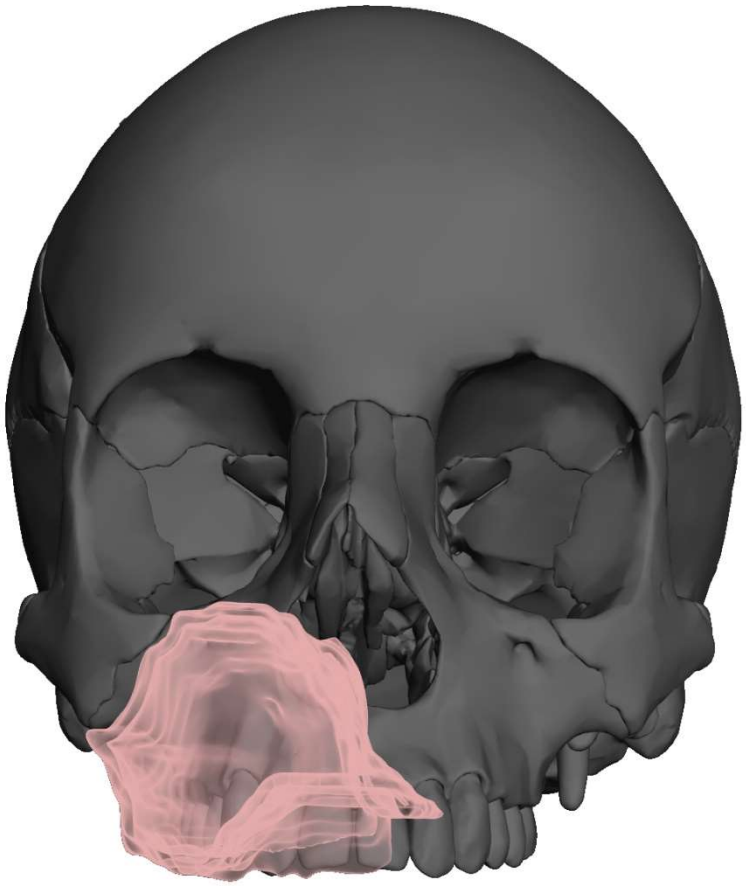

Master thesis

Technical Medicine

J. T. Ubbink

August 2019

UNIVERSITY OF TWENTE.

ANTONI VAN LEEUWENHOEK
NEDERLANDS KANKER INSTITUUT

Committee:

Chair and Technical supervision:	dr. Ir. F. van der Heijden
Medical supervision:	prof. dr. A.J.M Balm
Process supervision:	dr. M. Groenier
External supervision	ir. E.E.G. Hekman
Additional members:	drs. M. Krap
	dr. M.J.A. van Alphen
	dr. R.L.P. van Veen

Abstract

This master thesis provides the first steps towards the formulation of a digital design workflow for the production of a surgical obturator after maxillectomy.

The design of the current surgical obturator is not based on 3d delineation of the tumour and associated resection margins in CT and/or MR. This results in limited prior insight into the shape and extend of the defect that will be created during the maxillectomy procedure and prevents the presurgical production of a hollow surgical obturator. The surgical obturator is based on the intraoperative combination of a premade baseplate, which covers the defect, and a putty bulb, which fills the defect. The putty bulb is heavy which results in reduced patient comfort.

A digital workflow for obturator design aims to improve the obturator production time, reduce surgical time and increase patient comfort. A digital surgical baseplate was successfully planned, printed and evaluated parallel to the traditional design workflow. Evaluation of the relation between the traditional obturator bulb surface and the remaining bony skull segments shows that an undersized hollow obturator bulb leave a distance of four millimetres to the nearest bone segment.

These first steps show that the introduction of a digital workflow offers new ways of designing and producing obturators. However, it also shows the need for the introduction of digital delineation in the presurgical planning stage and illustrates the need for verification of results during and after surgery.

Table of contents

1. Introduction

1.1. Head and Neck cancers

With almost 3000 new cases a year, head and neck cancers (HNC) account for 2.7% of all new diagnosed cancers in 2015 in the Netherlands. The majority is of squamous cell carcinoma origin. Nine percent of these tumours are located in the maxillary region[1].

The maxilla is an ossified collection of bones of the skull. Ossification causes fusion of the skull bones with the maxilla being one of the final bones to be joined to the skull. It forms what is generally known as the upper jaw (figure 1). The maxilla provides a separation between the oral cavity and the maxillary sinuses and nasal cavity. Therefore, surgery of the maxilla has the potential to cause deformation to a patients' entire facial appearance if no adequate reconstruction has been performed.

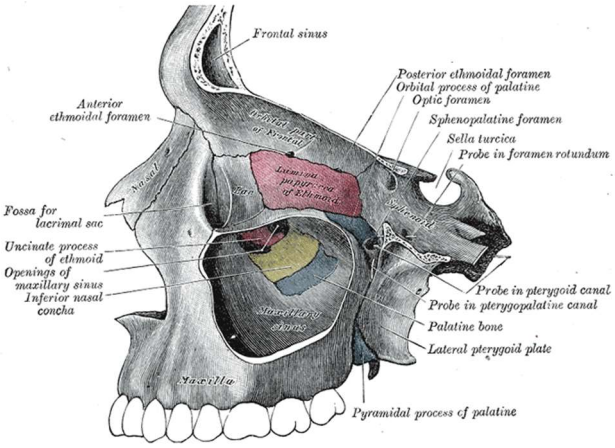

Figure 1: The maxilla, as seen from the side, with the left maxillary sinus opened. [40]

Carcinomas of the maxilla and palatum durum are primarily treated surgically[1], resulting in a two years survival of 76% and 71%, respectively. In T1 carcinomas, primary radiotherapy is an alternative treatment option. Surgery may also be followed by radiotherapy, in case of incomplete resection [2], [3].

1.2. Maxillectomy

Patients presenting with tumours in the maxillary bone (upper jaw) are often treated by surgical resection; a procedure known as maxillectomy. Depending on the extent of the maxillectomy, the tumour is approached via the mouth or through the skin. In the latter case, an incision is made from the eye, following the contour of the nose and bisecting the upper lip under the nose. This is called a Weber Ferguson incision[4].

The bones of the maxilla are bisected, following the intended resection margin, using a surgical sawblade and a chisel. Depending on the size of the created soft tissue defect, the soft palate and other structures may be closed by primary closure or closure using a Thiersch skin graft. The outer skin contour is restored by primary closure of the Weber Ferguson incision.

Due to the large variability in tumour locations and extensions, maxillectomy can mean anything from a small resection to large defect involving the whole midface region.

There are many classifications that propose a way of comparing the size of the defect created by maxillectomy[5]–[7]. A popular classification method was proposed by Brown in 2010 and can be seen in detail in figure 2. It combines a vertical extent measure (i-vi) with a horizontal extent measure (a-d).

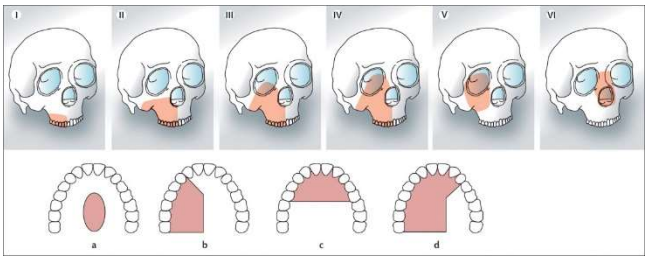

Figure 2: Brown's classification. Vertical classification: I—maxillectomy not causing an oronasal fistula; II—not involving the orbit; III—involving the orbital adnexae with orbital retention; IV—with orbital enucleation or exenteration; V—orbitomaxillary defect; VI—nasomaxillary defect. Horizontal classification: a—palatal defect only, not involving the dental alveolus; b—less than or equal to 1/2 unilateral; c—less than or equal to 1/2 bilateral or transverse anterior; d—greater than 1/2 maxillectomy. Letters refer to the increasing complexity of the dentoalveolar and palatal defect, and qualify the vertical dimension.[7]

When the surgical excision is finished, a defect remains. At this stage an obturator will be manufactured and fitted to the defect by a specialized maxillofacial dentist: the maxillofacial prosthetist. The eventual fit of the obturator depends on the shape and extension of the defect, localisation and remaining supportive structures in the skull bone. These variables may differ considerably among patients[8]. Patient comfort is significantly reduced by the resulting open connection between the nasal and oral cavities. This results in impairment of the functionality of speech, chewing and swallowing [9], [10]. Without defect reconstruction, long-term discomfort is caused by the collapse of soft tissue due to the absence of structural support from dissected bone[11].

1.3. Reconstruction

Reconstruction of the maxillectomy defect can be performed by a prosthetic obturator or free flap reconstruction using different bone segments from different anatomic sites[5], [8], [12].

There are several advantages to an obturator based approach[9]. Firstly, use of the obturator results in a smooth restoration of the hard palatal contour. Secondly, it promotes relatively normal speech, mastication and deglutition while also maintaining a patent nasal airway. Thirdly, by application of moderate pressure, collapse of the facial contour is prevented. Finally, the obturator allows for close inspection of the resection defect during follow-up and early detection of tumour recurrence with easy access for secondary surgical treatment. Optimal fitting of an obturator is a prerequisite and results in equivalent quality of life when compared to a surgical reconstruction using autologous bony tissue grafts[2], [9], [13].

1.4. Traditional design workflow

The current design and production process of the surgical obturator dates from the beginning of the twentieth century. During the first world war, military surgeons developed a lot of experience in fabrication maxillofacial prostheses to fill up large traumatic facial defects[14], [15]. Over the years, improvements of dental techniques and materials have resulted in a workflow that offers an optimal trade off in patient comfort, producibility, adaptability and cost. A schematic representation of this workflow can be seen in figure 3.

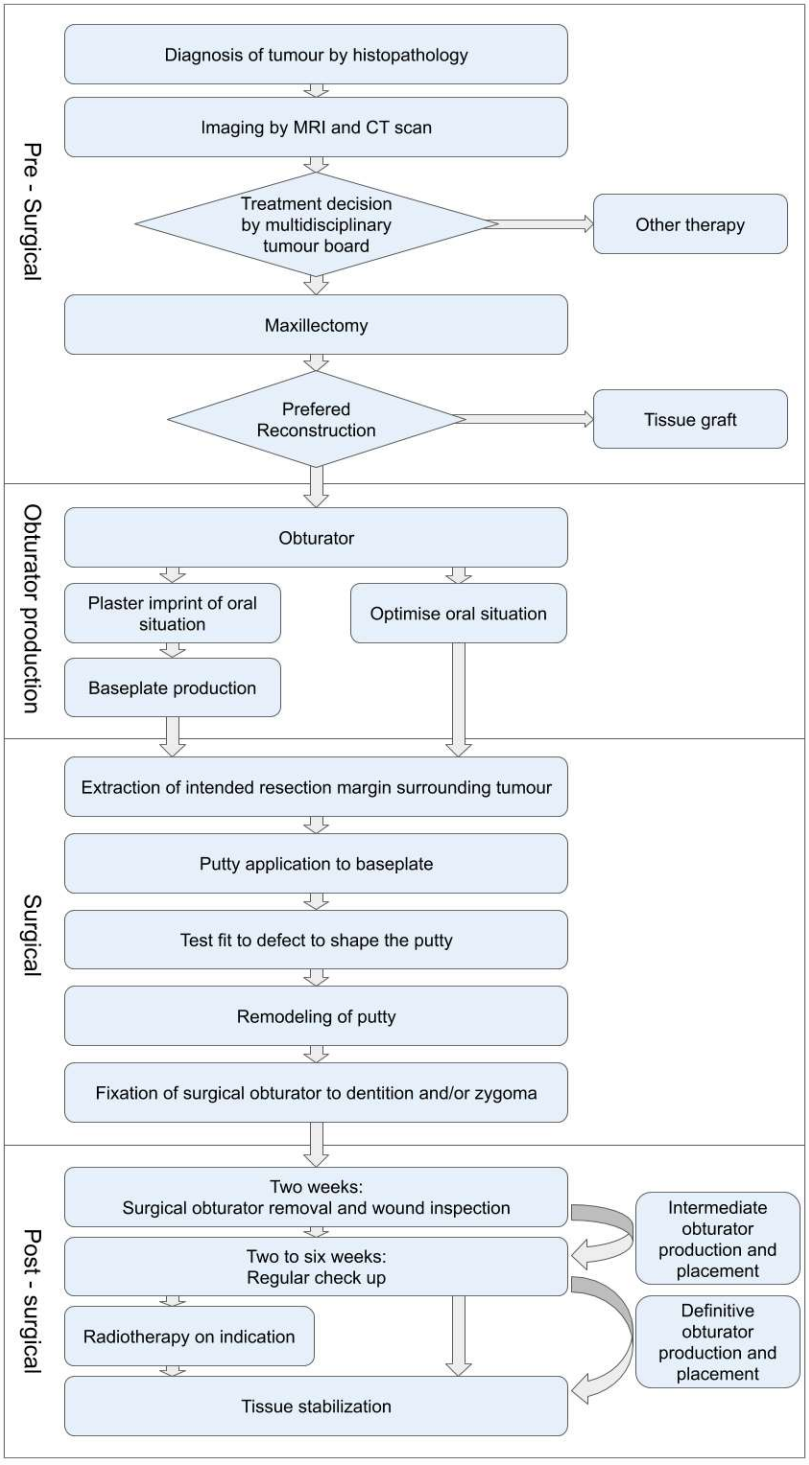

Figure 3: Traditional obturator workflow.

The traditional surgical obturator is constructed on the spot by merging a pre-produced patient specific baseplate with a bulb that consists of putty. The patient specific baseplate is manufactured out of hospital by a dental laboratory in the weeks prior to surgery. An imprint of the patients' dental and palatal state is used to produce an acrylic baseplate as shown in figure 4.

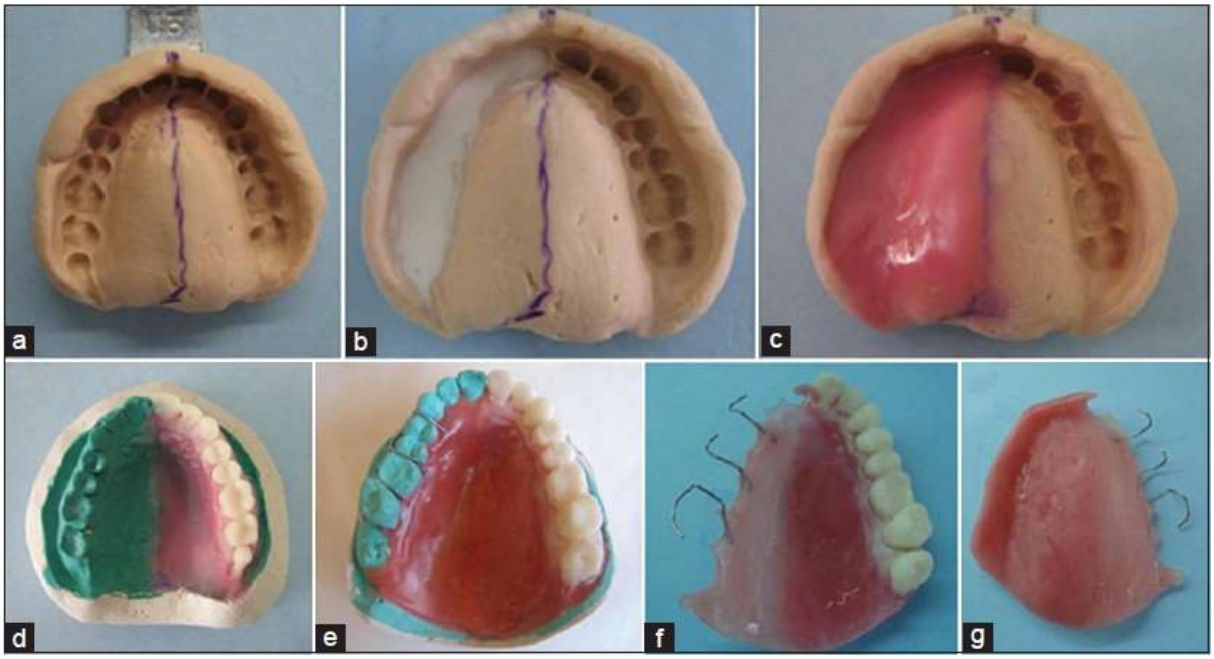

Figure 4: The production of the surgical baseplate(f,g) based on a plaster imprint of the presurgical dental state (a). Dental elements can be created using white acrylic resin to provide an aesthetically pleasing result(b). Alternatively, generic premade dental elements can be glued into position once the plate is finished. The baseplate is extended to fit around the remaining dentition and form a plate that covers the entire palate. Orthodontic clasps are cast into the acrylic resin to provide retention.(c-e). [16]

Orthodontic clasps are only used when healthy dentition is available on the contralateral side of the intended resection. This is essential as only healthy dentition can support the additional load that is applied by the obturator. If no dentition is available, zygomatic wires may be used, this will be further discussed in chapter two.

Putty is applied on the superior surface of the surgical baseplate to form the bulb that will fill the surgical defect. Putty is a polymer based material that cures over time due to addition of a catalytic hardening agent that is mixed with the putty prior to its application[17]. The amount of hardener that was added determines the amount of time available before the putty solidifies. An example of the baseplate with the putty bulb applied can be seen in figure 5. The combination of baseplate and putty bulb is called the *surgical obturator.*

The surgical obturator is primarily aimed at quick filling of the defect. It is not suitable to remain in place for long as the putty is porous, which allows bacterial infiltration, and it is heavy due to its solid nature. When the wound has healed and stabilised it is replaced by an intermediate obturator that is fully composed of acrylic resin. The intermediate obturator may require modification in case of changed tissue shape due to the healing process in the months after surgery. Once the surgical defect has healed and the soft tissue has fully stabilised, the intermediate obturator is replaced by a definitive obturator.

Figure 5: Surgical obturator with pre-produced acrylic baseplate (transparent) with retention clasps and putty bulb (blue). [18]

The primary aims of obturator based reconstruction are:

1. Providing immediate replacement of functional loss following surgery by providing obturation, occlusion, retention and stability.
2. Reducing impairments of deglutition, speech and mastication.
3. Preventing cosmetical changes to the midface due to fibrosis and lack of bony support.

The traditional surgical obturator meets these requirements adequately in small defects. However, when the extent of surgery increases to higher Brown class defects, the production of an obturator that performs adequately is more challenging.

During the surgical procedure, the maxillofacial prosthetist is confronted with the final defect after the maxillectomy. The shape and placement strategy of the prosthesis should therefore be performed on the spot with unexpected last minute time consuming adaptations as a result.

The required shape of the obturator bulb is highly patient specific. This is mainly caused by the large variation in tumour extensions. The resulting types of defects following maxillary surgery have been described in various classifications as mentioned before. However, these classifications intend to report the extent of surgery and cannot be used for an exact pre-surgical planning of obturators. They lack quantifiable tissue borders, which have to be applied to individual patients. In order to produce a patient specific obturator, accurate presurgical planning of the surgical defect is required. A digital design workflow is required to achieve this. Such a digital workflow has not been developed until now.

1.5. Digital design workflow

Over the past years, advances in the fields of computer aided design (CAD)[19], [20], additive manufacturing (AM)[21]–[23], and virtual surgical planning (VSP)[24], [25] have been implemented in medical practice and offer new ways of design and construction. This can potentially change the way maxillectomy and obturator production are performed in the future.

Recently, the evaluation of maxillectomy resection borders utilising intraoperative cone beam computed tomography (CBCT) has shown to be usable to determine the conformity to presurgical planning[26]. This provides a way of evaluating the defect size, which may contribute to the

introduction of image guidance in maxillectomy in the near future. This is expected to improve the conformity of the resulting surgical defect to the pre-surgical planning.

Digital design can assist in the patient specific production of an obturator, while also allowing partial pre-fabrication of the obturator. When an obturator is printed pre-surgically, it is essential that it fits closely to the remaining tissue once the surgical defect is made. This is more challenging since accurate prediction of the defect depends on numerous anatomical variations that introduce uncertainty into the equation.

The increased predictability of defect borders, resulting from image guidance, will allow modification of the obturator production from an analogue process to a digital workflow. The future obturators may be produced as single piece product instead of the traditional baseplate and putty bulb as a result of additive manufacturing. For practical reasons, the digital design of the obturator is still subdivided into two design stages: The *surgical baseplate* and the *bulb.*

1.5.1. Surgical Baseplate

The surgical baseplate has several functions. Firstly, it provides separation of the oral cavity and the surgical defect. Secondly, it provides a way of securing the obturator to the patient. Finally, it transfers the forces of mastication to the bony support. Therefore, a digitally designed baseplate should be comparable to the traditional baseplate. Furthermore, the surgical baseplate provides a foundation from which the bulb is extended into the maxillectomy defect. Therefore, accurate digital planning of the bulb requires the availability of an accurate digital representation of the baseplate during the planning stage.

1.5.2. Bulb

One prerequisite for the digital design of the obturator to be used during surgery is a proper fit of the obturator to the surgical defect. The surface of the obturator bulb is in close proximity to the resection margin as it aims to fill the void that is left after excision of the tumour. Therefore, the accurate prediction of the distance over the entire surface between bulb and remaining surrounding tissue is essential for the successful presurgical planning of the size of the obturator bulb. Due to unexpected extensions of excision margins during surgery, under sizing of the bulb is preferred as this can be compensated with the application of a soft lining material.

Soft lining materials have been used extensively in dental applications[27], [28]. They are often silicon based and provide a soft layer between a hard acrylic denture base and the patients' soft tissue. The primary goal of soft liner material application is to absorb energy and spread mechanical load[27]. In this case, the material is applied on the surface of the under sized obturator bulb to provide a seal between the acrylic obturator bulb and the remaining soft tissue and bone (figure 6).

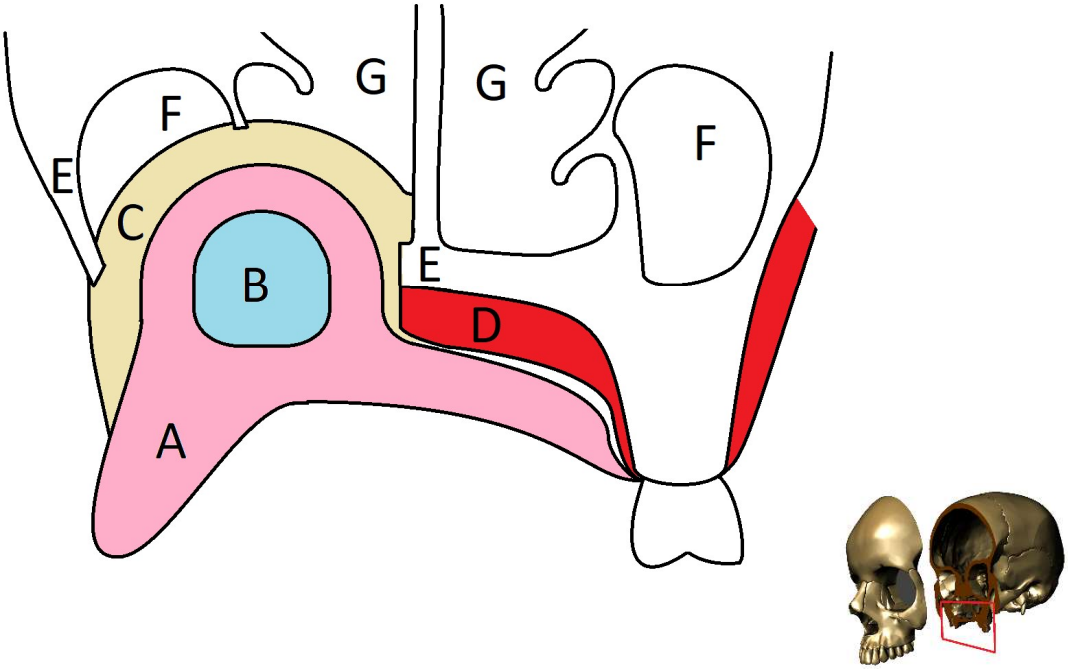

Figure 6: Coronal view of the maxilla, after maxillectomy, with obturator (A), hollow bulb (B), and soft lining material (C). The obturator is undersized to allow accurate fit. The soft lining material fills the void between obturator and the soft tissue (D) and bone(E). The maxillary sinus (F) and the nasal sinus (G) on the defect side are partially filled by the obturator.

The amount of under sizing that is required for the bulb to fit is currently unknown. Therefore, quantification of the distance between the remaining supportive bony segments of the skull and the traditional obturator surface is required to provide insight into the required bulb dimensions that will allow the optimisation of presurgical digital design of an obturator.

1.6. Aim and research questions

The ultimate aim of the current project is to obtain a digital workflow that (a) provides reduced obturator production time, (b) provides reduced surgical time and (c) increases patient comfort. The current study aims to identify and implement the first steps towards the formulation of such a workflow.

The main research question is: How can digital pre-surgical planning be introduced in the obturator design workflow?

In order to provide the first steps to answering this question, the following sub questions will be addressed in this study:

1. *To what extent is the digitally designed surgical baseplate identical to a traditional surgical baseplate?*
2. *What is the acceptable closest obturator distance to the remaining bony structures, which allows optimization of a presurgical design of an obturator?*

1.7. Study and thesis outline

This thesis continues by addressing the two sub-questions in the following chapters.

The comparability of a digital designed surgical baseplate to a traditional design surgical baseplate is described in chapter two.

Chapter three focusses on the distance between the obturator bulb and the remaining bones of the skull.

Chapter four summarises the results from the previous chapters and describes how the bulb and baseplate may be combined to form an one piece obturator that can be produced using additive manufacturing in the future.

Chapter five provides further elaboration into the clinical implications and the future perspectives. It also describes the limitations that currently limit the introduction of a digital design workflow and elaborates on the possible ways these limitations can be overcome. This leads to an advice that may accelerate the introduction of a digital design workflow.

2. A proposed design-workflow for digital obturator baseplate design

2.1. Introduction

The baseplate is an important component in the production of the surgical obturator. It provides contact and support by closely following the contour of the gingival tissue and dentition. The baseplate provides a platform from which the obturator can be extended into the surgical defect. Furthermore, fixation of the surgical obturator can be achieved with surgical wires passing over the zygomatic bone or around remaining dentition (figure 7).

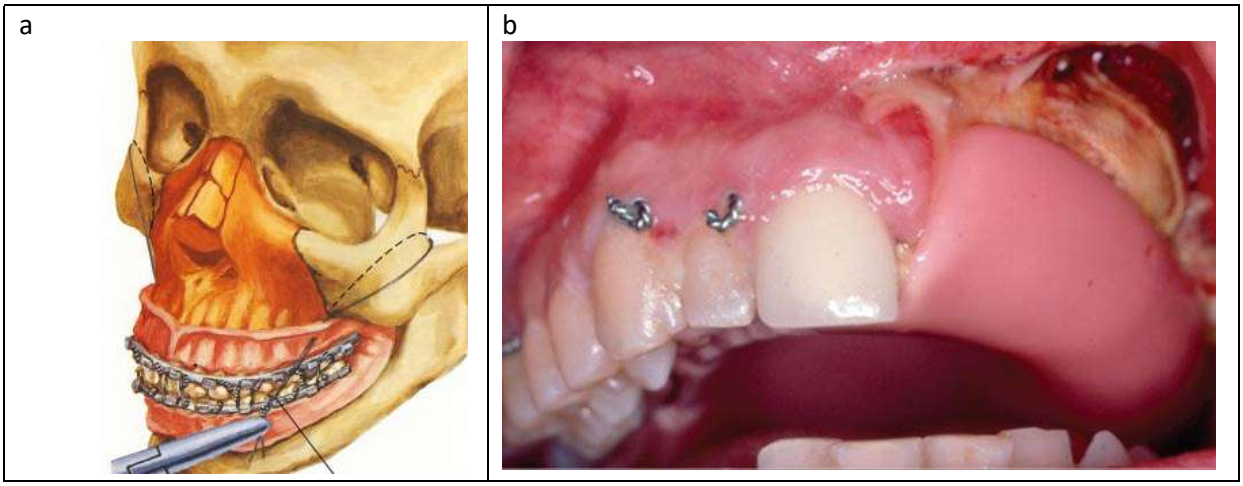

Figure 7: Illustration of fixation using zygomatic wire(the black loop) (a) and dental wire(b)[29]

Currently, the baseplate is produced from a plaster cast of the patients' pre-surgical dental state as was previously described in chapter one. The introduction of resins for additive manufacturing can be used in the production of dental prosthetics. These materials have been tested and approved for use in human application and have found their way into dental and medical practice [20], [21], [30].

The oral imprint is a technique that is still used extensively because of its widespread availability and low cost. Over the past years, intra oral scanners have shown to be a good alternative to imprints with superior accuracy and patient comfort as reported advantages [31]–[34].

Currently, we are looking into the possibility to introduce virtual planning into a future workflow for the production of obturators. A virtually designed obturator will require the availability of a digital surgical baseplate as a platform for the connection of a digital design bulb. This is essential as a good fitting baseplate provides increased stability and promotes proper separation between the oral and nasal cavity.

The goal of this project is to design a digital baseplate from scratch by formulating a workflow based on expert opinions. Design requirements were formulated in close consultation with a maxillofacial prosthetist and surgeon. Once the design is finished, it is compared to the traditional baseplate that has been produced by the dental laboratory and was designed independent from the digital workflow. This provides the first insight into the feasibility of digital design of an obturator baseplate. The question this chapter aims to answer is:

To what extent is a digitally designed baseplate identical to the traditional baseplate?

2.2. Materials and Methods

2.2.1. Data

This single-case study was performed in parallel to the traditional production of a surgical baseplate during the weeks leading up to maxillectomy.

2.2.1.1. Intraoral Scanner

A plaster cast of the patients dental status was scanned using a Trios 3Shape intraoral scanner (3Shape, Copenhagen, Denmark). The reported accuracy of the Trios 3shape is 50 µm [31], [33], [34]. Scanning was performed according to the suggested protocol supplied by the manufacturer. In the protocol, the occlusal plane of the dental arch is scanned first. This is followed by consecutive sweeps adding information of the buccal and lingual sides of the arch to the model. This is illustrated in figure 8. The generated model is visualised in realtime while scanning. Therefore, the operator can observe where data is missing and actively scan these areas. Image and feature matching is used to stitch a new set of datapoints to the previously recorded data. The scanner produces a digitized representation of the plaster cast that is exported as a surface tessellation language (STL) file.

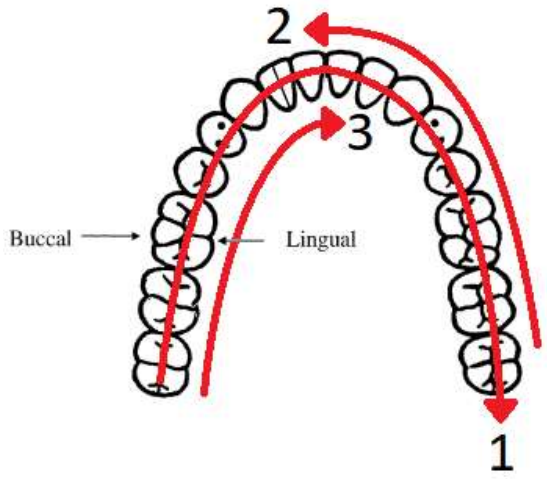

Figure 8: Intraoral scanning protocol. Sweep of the occlusal arch (1), buccal (2) and lingual (3) sweeps are used to add data to the model.

2.2.1.2. Digital representation of surfaces with faces and vertices.

Digital models are composed of vertices and faces. Vertices are points in three-dimensional space with a x-, y-, and z-, coordinate. A face is the combination of three or more vertices. Triangular faces are used in this study, therefore a face can be described as a triangle with three vertices on its edge. The face normal is directed perpendicular to a face and points in the direction the face is facing. This is illustrated in figure 9.

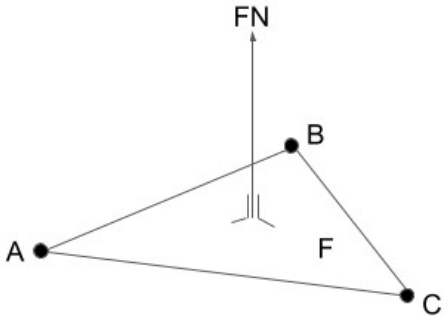

Figure 9: schematic representation of a face (F), composed of three vertices(A,B,C), and the face normal perpendicular to the face (FN).

Multiple faces can be connected to form a complex surface. In this case each edge of a face overlaps with the edge of an adjacent face to form a network of faces.

2.2.1.3. The delineation of tumour and intended resection margin

CT and MR images of the patient are acquired in DICOM file format. The CT and MR images are registered using the Elastix package[35] available in 3DSlicer[36]. The dentition and tissue-to-air border can be more accurately determined in the CT images. The intra oral scan model is fitted to the CT data manually. The MR imaging is used to delineate the border of the tumour and the intended resection margin which will be used as an indication for the extension of the posterior edge of the baseplate that is required to cover the surgical defect.

2.2.2. Design requirements for the digital obturator

Expert opinion in combination with the current gold standard surgical baseplate was the inspiration for the formulation of the following design requirements for the digitally designed baseplate:

- In order for the plate to be strong and rigid, a minimum thickness of 2mm is formulated. This also lowers the risk of printing errors by preventing the occurrence of thin areas.
- In this individual case the traditional surgical baseplate has steel clasps that clip around the remaining dentition. These clasps can be added to the digitally designed baseplate once it has been printed. Two 1.5mm diameter holes are designed to facilitate wire fixation around the two upper canine dental elements (13 and 14).
- A close fit to the teeth is required to achieve placement of the plate without play. Thus, preventing instability of the plate. Therefore, only light smoothing is applied to the gingival contact area of the baseplate.

2.2.3. Digital design workflow

The digitized plaster cast is used as a base which is manipulated to design a digital plate by following a cascade of operations in Meshmixer which has been visualised and described in figure 10.

1. The face normals of the surface are facing inwards as the plaster cast is inversed compared to the anatomical situation. The face normals are flipped in order to produce an exterior facing surface that represents the anatomical situation.	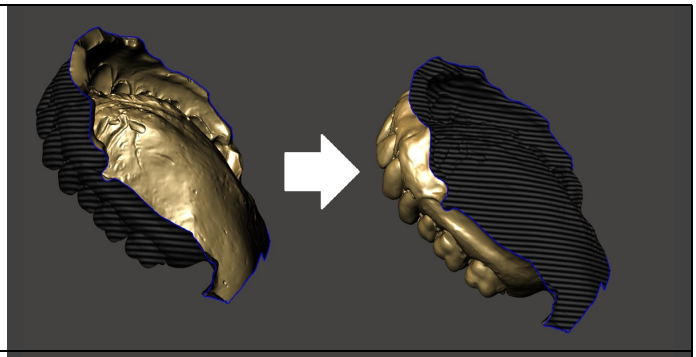
2. Selection of oral mucosa of palate. The tissue-to-teeth border is followed using a manual selection tool. This selection is extended visually to a full selection of the palatal mucosa and separated from the non-selected parts of the intraoral scan data.	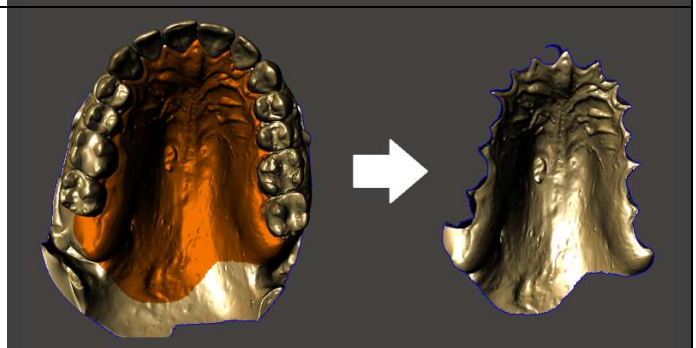
3. The surface currently consists of two-dimensional faces and can be considered as a layer that is warped in a three-dimensional world. However, the thickness of the layer is not defined due to the two-dimensional nature of a layer. In order to transform the layer into a three-dimensional volume, the surface is extruded to a thickness of 2mm. The extrusion is performed with one degree of freedom in caudal direction. This guarantees that the shape of the obturator is only modified in this direction. This prevents expansion in a sideways direction, which would result in interference of the plate with the teeth.	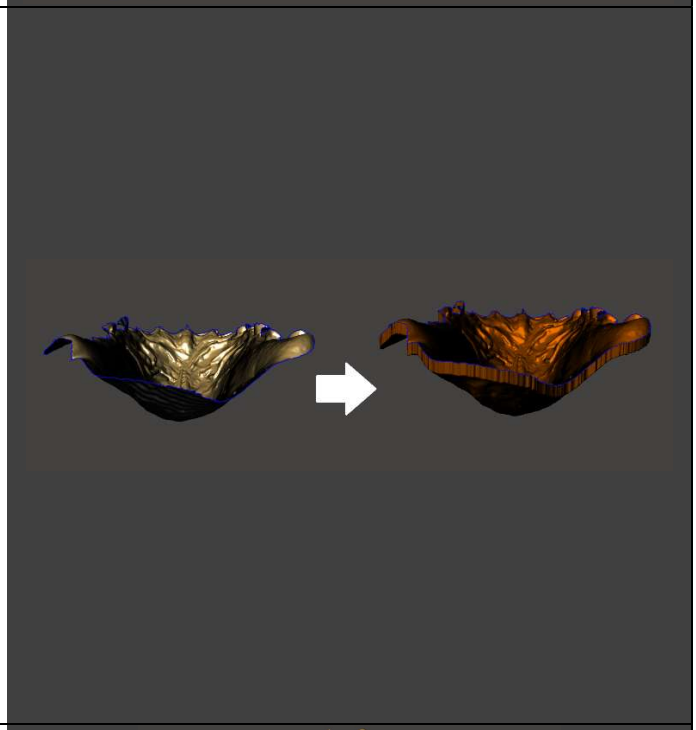
4. The rear facing border that is created this way can be extruded in posterior direction to extend the plate to cover the intended resection defect. The tumour outline and intended resection margin are used as a guide to determine the shape of the rear border.	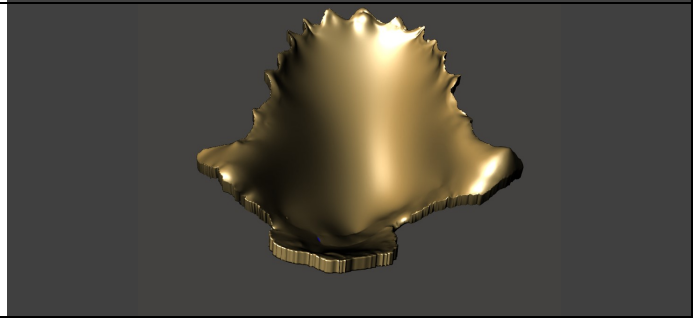

The inferior edges of the obturator are rounded using a smoothing tool. The inferior surface of the obturator is smoothed. The rounding and smoothing prevents sharp extensions of the baseplate that may damage the tongue.	
5. A mushroom shaped extension is added to the superior surface of the obturator to facilitate retention of putty to the baseplate. It is positioned to protrude into the centre of the intended resection defect. Holes with a diameter of 1.5mm are added for wire fixation. The smoothing of the inferior surface has caused the centre of the inferior plate to be too thick. This is corrected by hollowing until the plate thickness of 2 mm is restored.	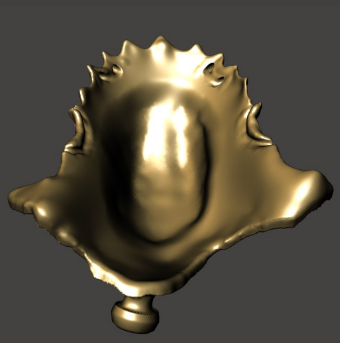

Figure 10: The step-by-step design of the digital baseplate.

2.2.4. Virtual test fitting

Once the traditional baseplate is delivered from the dental laboratory, it is scanned using the intraoral scanner. It is exported as an STL file. The scanned traditional baseplate is compared to the digitally designed baseplate. First, both models are registered using the iterative closest point (ICP) algorithm[37]. This algorithm aligns two sets of points, or baseplates in this case, to achieve optimal overlap of their morphology. Next, the distance between the vertices of the two models is calculated using a method that is covered extensively in section 3.2.2. In short, for each vertex of one model the closest vertex on the other model is selected and the distance calculated. This results in a distance map that shows the difference between the surfaces. If the virtual test fit shows good agreement between the digital design and the traditional design, the next step is to 3D print the digital plate and test fit it to the plaster cast.

2.2.5. 3D Printing

The baseplate is printed using a Form2 (Formlabs, Somerville, US), a Stereo Lithography Apparatus (SLA) 3D printer. SLA type printers produce objects by stacking layers of curable resin. The build platform is lowered into a reservoir filled with uncured resin. The outline of the layer is traced by a 250 mW laser with a wavelength of 405 nm. The resin solidifies locally when it is illuminated by the laser light. The print is post cured using UV light. The Form 2 can be used to print Class I biocompatible resin (DentalSG) that has been FDA approved for use in dental applications. Objects printed with this resin can be sterilised which makes the prints applicable for use in clinical and surgical cases.

2.2.6. Verification of fit

The printed plate is fitted to the plaster cast. Design choices that have been made in the digital design stage may prevent the plate to fit accurately which will show during this fit. In this case, the feedback from this test is used to make adjustments in a new iteration of the design. In case of a confirmed fit and conformity to the traditional baseplate, the digital design traditional baseplate printed plate will be sterilised and test fitted in the patient during the surgical procedure.

2.3. Results

The traditional baseplate and the digital designed baseplate show differences in their appearance (figures 11a and 11b). The traditional design baseplate extends further backwards to cover a larger portion of the intended surgical resection. In addition, it lacks the wings that surround the posterior portion of the second molars that can be seen in the digitally designed baseplate in figure 11c. Another clear distinction that can be made between the two baseplates are the steel clamps that are present in the traditional design baseplate.

Comparison of the overlapping parts of the traditional baseplate and the digitally designed baseplate shows a median distance of 0.453 mm and a mean distance of 0.476 mm (table 1). Several red spots can be seen on features of the baseplate that extend from the surface of the baseplate (figure 11d and 11e).

The results from the virtual test fit and the test fit of the 3D printed digital designed baseplate to the plaster dental model, provided confidence that the printed plate would also fit in vivo (11f). This was confirmed by a successful placement of the traditional baseplate printed digital designed baseplate following the maxillectomy (figure 11g).

Mean	0.476 mm
Sd	0.212 mm
Min value	0.0147 mm
Median value	0.453mm

Table 1: Vertex distance statistics

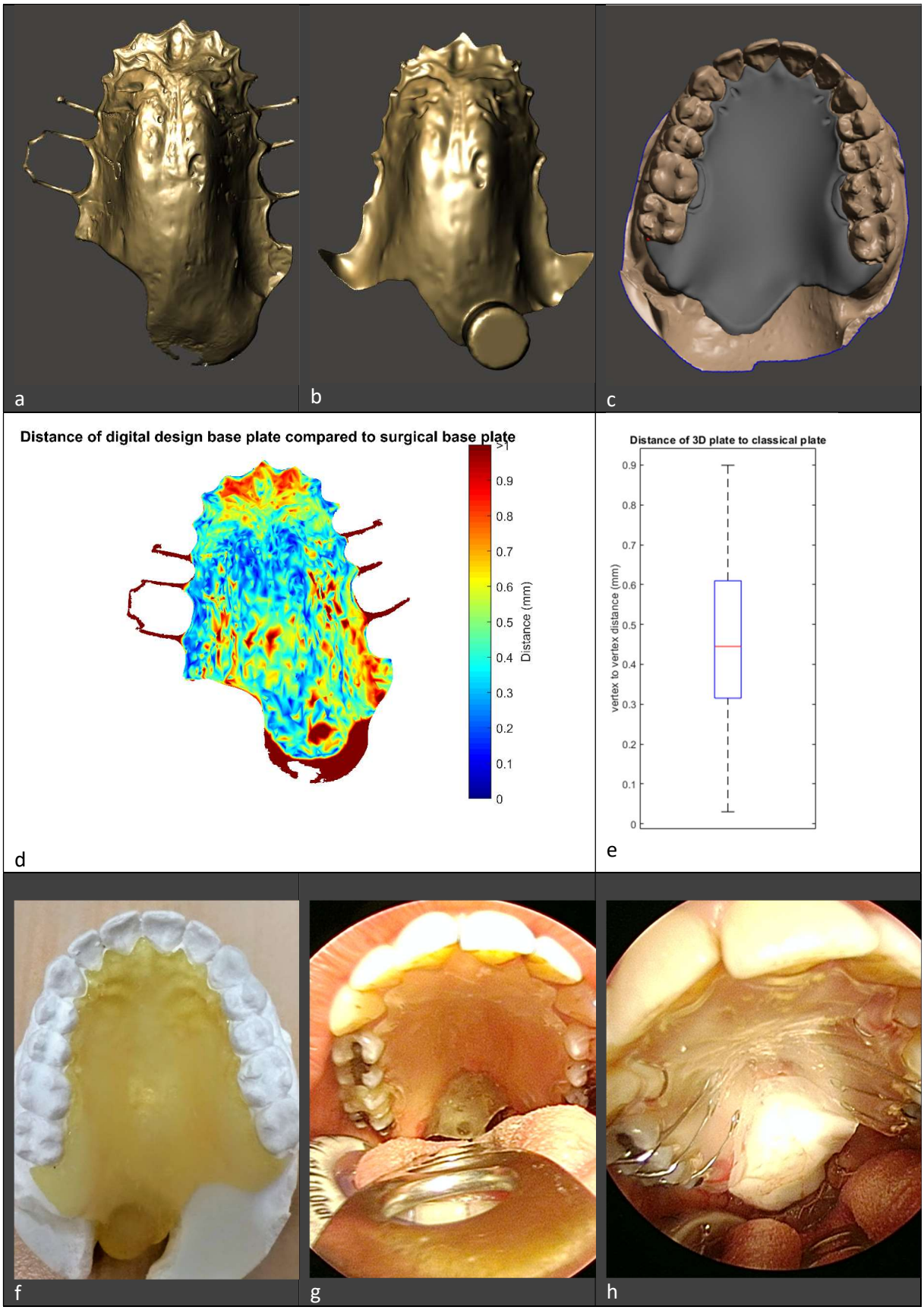

Figure 11: Traditional surgical baseplate (a), digitally designed baseplate (b), plaster cast with digitally designed baseplate with the mushroom extension (c). Distance map between traditional surgical baseplate and digital design base (d), boxplot of vertex-to-vertex distances. (e), Light photo of the plaster cast with 3D printed digitally designed baseplate (f).Digitally designed baseplate, in vivo (g). Traditional design baseplate, with putty bulb in white, in vivo (h)

2.4. Discussion

Deviation differences between the two plates may arise from differences in measurement errors. The intraoral scanner was used to scan the plaster cast and the surgical baseplate. Literature reports an accuracy for the Trios 3Shape intraoral scanner of 9 µm in controlled in-vitro experiments and up to 50 µm in in-vivo scanning[33]. The surgical baseplate is constructed from acrylic resin and was finished by polishing which made successful completion of the scanning procedure noticeably harder.

Inaccuracy in the production of the surgical baseplate may contribute to the deviation. Several steps of casting and releasing of moulds introduce a cascade of inaccuracy in every step. The finished product is test fitted on the plaster cast to confirm conformity with the anatomy of the patient. The intraoral scanner combined with a digital design workflow may greatly reduce the deviation from the anatomical situation due to a limitation of this type of errors.

The reported distances show an average distance of 0.4 millimetres. Differences up to 1 millimetre can be accommodated by the soft tissue of the palate which suggests that no functional limitations are to be expected from the observed differences. Closer inspection of the digitally designed baseplate shows the smoothing that has been applied during the design. This explains the larger differences that are observed in the extending features along the baseplate surface.

A limitation of this research is the use of the plaster cast as input. At the time of baseplate production, the intraoral scanner had not yet been approved for clinical use. This meant that the less favourable option of scanning the plaster cast had to be performed. Ideally a scan of the patient anatomy is to be used as this excludes the inaccuracy of the plaster cast from the error cascade.

The steel clasps cannot be incapsulated in the digitally designed baseplate during the traditional baseplate printing as this would interfere with the resin. Therefore, they will need to be added after the baseplate has been printed. However, it is possible to include the required position of the clasps during the digital planning of the baseplate. This would result in the planning of recesses in the plate at the intended location of the clasps. The clasps can be positioned in these recesses and fixated using biocompatible glue.

A clear difference between the traditional baseplate and the digitally designed baseplate can be noticed when comparing the shape of the posterior border of the plates. This illustrates the difference that may arise when the obturator is produced externally and may be contributed to personal preference or limitations of the production process.

This study shows that the differences in baseplate construction are mainly determined by the choices that are made during the design process and not by the accuracy of the digital design workflow. Therefore, the definition of additional design criteria is required to improve the reproducibility of the design. At first these criteria could be based on the criteria of the current baseplate design. However, it is expected that digital design and manufacturing will offer many new ways to design and produce a baseplate. This may result in design criteria that are specific to digital design. That is the moment when the production of an identical baseplate should no longer be the goal of digital obturator production.

Introduction of the digital design workflow may be used to produce a standardised way of baseplate production. It may introduce a way of documenting and identifying design considerations that can be specific for both patient and the manufacturer/designer.

2.5. Conclusion

Digital design of the baseplate has been shown to be an alternative to the current way of baseplate production. The digital workflow proposed in this study was used to design a baseplate that shows agreement between the traditional plate and the proposed plate with a mean distance between the surfaces of the designs of 0.47 mm ± 0.21 mm. Differences were seen in the inferior extension of the plate and in the baseplate surrounding the M2 elements. These differences did not limit the physical fitting of the digitally designed baseplate in the patient. This first try at designing a digital baseplate shows that it has the potential to be designed identical to the traditional baseplate if further design criteria are formulated.

3. The distance from remaining bone segments to the surface of the obturator bulb

3.1. Introduction

The obturator surface has a close relation to several segments of the skull as can be seen in figure 12. The shape and dimensions of the obturator are distance related to the surgical defect created during maxillectomy. This close relation is essential to create a patent seal between obturator and the remaining soft tissue. In addition, an obturator of proper dimensions will increase the total contact area between tissue and obturator. This will provide the patient with a more stable fixation by providing more points of contact between the obturator and remaining supportive bone structures. Larger contact areas will provide spreading of the mechanical load that may result from e.g mastication. Pressure points due to tissue compression may arise over time when the obturator exerts pressure locally. Pressure points may result in discomfort due to pain and consequent swelling may cause the fit of the obturator to degenerate.

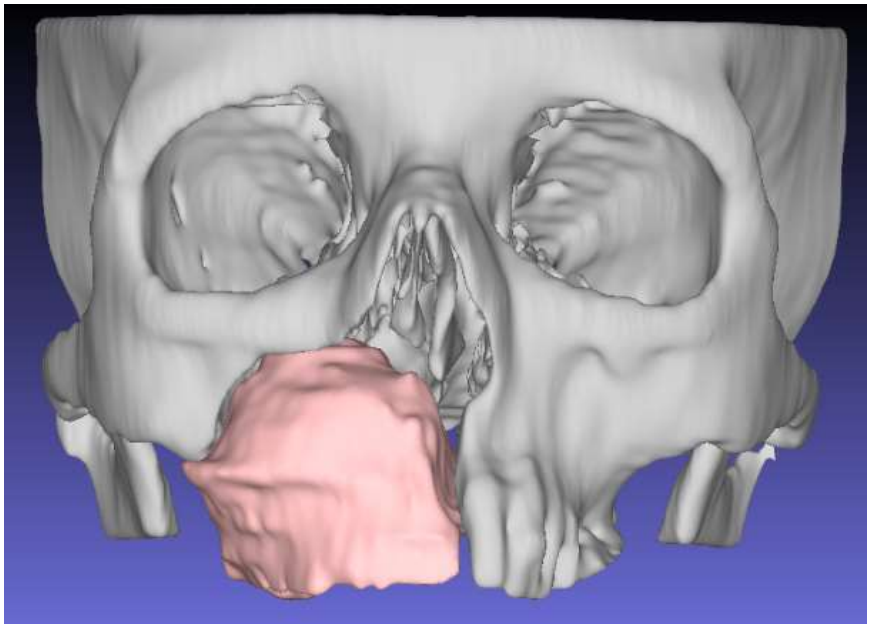

Figure 12: The segmented surgical obturator and skull show the close relation of an obturator to the remaining bone of the skull

The complex shape of the obturator bulb is currently guided by the surgical defect when the putty is put in place. The maxillofacial prosthetist can roughly mould the shape of the bulb by varying the amount of putty on the surgical baseplate. Once the baseplate is inserted, the remaining tissue and bone will provide resistance to the flexible putty and cause it to deform into a shape that follows the edges of the defect. The putty will protrude into air spaces like the nasal cavity and oropharynx. This may result in obstruction of the patent airway or irritation of tissue that causes swelling post surgically. Therefore, these undesirable pieces of putty are removed directly after moulding of the putty and prior to the final insertion and fixation of the obturator.

The traditional bulb production technique described above, can be classified as ‘safe by design’. The putty will deform if it is pressed into bone supported soft tissue when it is still flexible. However, this may change over time when the tissue changes shape due to initial swelling after surgery and due to

general changes in shape caused by wound healing and fibrosis. External mechanical loading due to mastication by the patient may also cause the formation of pressure points.

Currently, 3D CT/MR based delineation of the surgical margin is not standard protocol. Visual inspection of CT and MR provides a general indication of the expected shape, dimensions and anatomical localisation of the surgical resection. However, these intended margins may differ once the tumour is resected. Possible limited visibility of the tumour in the pre-surgical imaging and progressive growth of the tumour in the pre-surgical work-up stage can result in the neglection of the intended resection margin.

3.1.1. The digital workflow

Non-visibility and possible progression of the tumour makes digital design of the obturator vulnerable to design induced misfit. This may occur when the digitally designed obturator is based on an incorrect interpretation of the MR/CT data. As a result, such an obturator leaves no room for per-surgical modification to generate a good fit.

Additive manufacturing of the obturator aims to produce a rigid object that can handle the forces applied on the obturator. Once manufactured, the additive manufacturing obturator should not require modification during surgery as this is labour intensive and time consuming. Tumour growth during waiting time before surgery means that, in general, the defect appears to be larger when it is approached during surgery. Ideally, the pre-produced obturator is small enough to fit into the intended resection. Additional extension with a soft lining material can provide the required contact with the surrounding tissue. The soft lining material can be corrected or moulded easily in order to correct for possible differences between the pre-planned surgical margins and the actual surgical margins (see figure 6).

The current gold standard method of shaping the putty, using the remaining tissue of the defect as a mould, can be emulated in a digital design workflow. In this case, the amount of space required to allow the application of an outer shell of soft lining material is applied onto the obturator. Next, it is introduced into the defect where the soft lining material is shaped by anatomical structures that remain in place after surgical resection.

The distance between the outer surface of the obturator bulb and the remaining bone of the skull can be determined in post-surgical CT scans of patients that received a traditional surgical obturator. Evaluation of these distances can provide insight into the desired distance, from bone to obturator surface, that is currently achieved in traditional surgical obturator production. And may be indicative for the distance that has to be taken into account in a digitally designed obturator.

A hollow bulb is desired in order to reduce the total weight of the obturator. The production of a hollow bulb surgical obturator is one of the future developments that is thought to provide a large increase in patient comfort as this results in a surgical obturator with a lower weight. Therefore, Identification of the distances between the obturator surface and its nearby bone segments can lead to the formulation of a generalised distance that can be taken into consideration as a design parameter in the presurgical digital design of the bulb.

This raises the following question that is addressed in this chapter:

what is the acceptable closest obturator distance to the remaining bony structures, which allows optimization of the presurgical design of an obturator?

3.2. Materials and Methods

3.2.1. Data selection

In order to evaluate the relation between the obturator surface and the remaining bone of the skull, post-surgical imaging data is required. Five patients that were provided an obturator after maxillectomy surgery, were selected in consultation with the maxillofacial prosthetist. These patients were assessed according to the following inclusion criteria:

- Received Post-surgical radiotherapy and CTRT imaging .
- Hemi-maxillectomy of Brown class II-a or II-d. (see figure 2)

After surgery, the pathologist evaluates the tumour resection margins of the extracted maxilla segment. If the margins are not free from tumour cells, post-surgical radiotherapy of the defect is administered as additional treatment. CTRT scans are made to allow planning of the radiotherapy. However, these scans also provide an opportunity to analyse the obturator and surgical defect.

Hemi-maxillectomy patients were selected, as this is a common group of maxillectomy patients that is treated with an obturator. The inclusion of a group of comparable maxillectomy class patients aims to generate a dataset of comparable patients. This may promote the identification of common bony areas and distances for this class of maxillectomy patients. Different Brown classes may have specific bone areas and obturator surface to bone distances of their own.

The acquired CTRT scans had voxels of size 0,97mm x 0,97mm x 1,5mm. The scans were made an average 37 days post-surgery. The patients had already received an intermediate obturator by this time. As a result, the obturator may have been modified due to uncomfortable fit and/or soft tissue transformation as a result of healing of the defect. Unfortunately, this has to be accepted as no further scans are available. Four patients were treated with a class II-b maxillectomy. One patient was treated with a class II-d maxillectomy, which crossed the anterior-posterior midline of the hard palate. In one patient the tumour was located on the left side, whereas the others had a tumour on the right.

3.2.2. The identification of bone segments that are close to the obturator surface

The segmentation of groups of faces on the obturator surface that have a close relation to bone segments of the skull is implemented into Matlab. A cascade of several steps is described that together result in the identification of bone areas that show a small distance to the obturator surface. Before each step is covered, an overview of the cascade is given in figure 13.

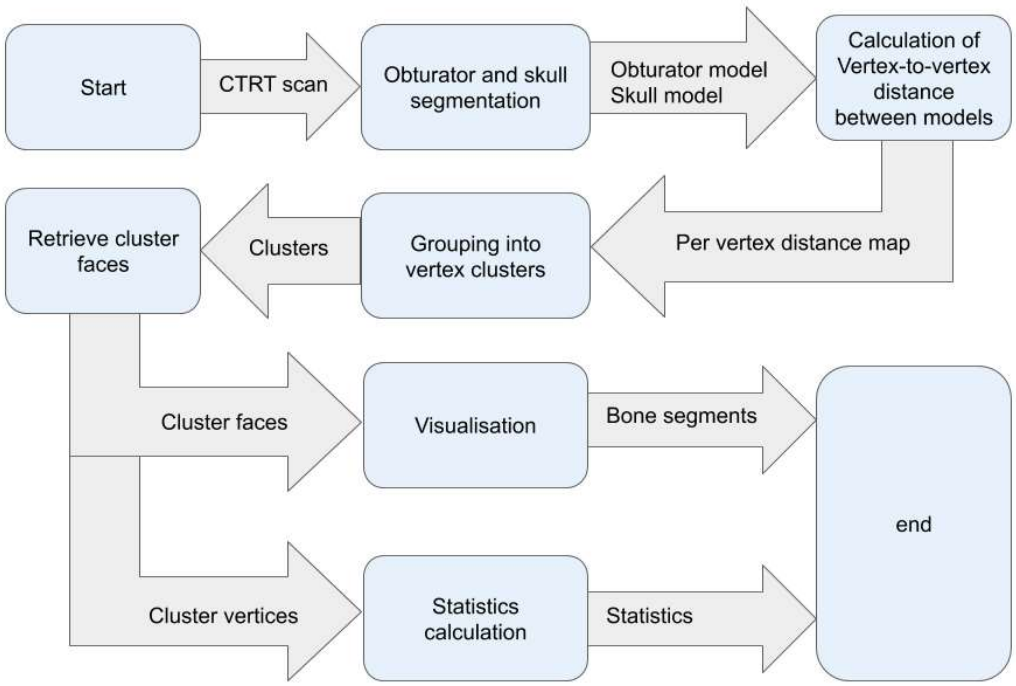

Figure 13: Flowchart describing the steps performed to go from CTRT scan to identified bone segments and related statistics. Blue boxes show the operation that is performed and relate to the subsections 3.2.1 thru 3.2.5

3.2.1. Obturator and skull segmentation

Three software applications are used to process the CTRT scans.

- 3DSlicer[36] offers a wide array of tools and plugins for medical image processing. It is used to segment the CTRT scans with the thresholding tool and with the manual segmentation tools. The segmentations are transformed to models and exported as triangular meshes in the STL file format. These meshes consist of a list of vertices and faces. A vertex is a vector containing three coordinates. These coordinates are the x, y and z coordinate of a point in three-dimensional space. Three vertices can be connected to form a triangle or face. Further graphical reverence can be found in figure 9. Triangular meshes consist of many connected faces which allows the representation of complex shapes such as the obturator and the skull. The coordinate system of 3DSlicer is defined in millimetres. This is retrieved from the CTRT DICOM voxelsize metadata. The vertices of the triangular mesh are therefore also in millimetres.
- Post-processing is performed in Meshmixer[38]. This is an application that offers tools to manipulate triangular meshes. It is used to close holes in the skull- and obturator models that are remained after the thresholding in 3DSlicer. Some models had interior surfaces that remained after hole closure. These surfaces were removed in order to have obturator models that only have a closed exterior surface.
- In order to check the conformity of the models to the CTRT scans, the models are reloaded into 3DSlicer where they are superimposed onto the CT slices. As the coordinate system has not changed, the three-dimensional obturator model will ideally intersect the slice exactly at the edge of the segmented anatomy. The model is traced thru the CT and visually evaluated for accurate segmentation.

- Matlab R2018b[39] was used to develop an algorithm (pseudocode in figures 14 thru 16) to analyse the distance between the surfaces of the resection margin and the obturator surface.

3.2.2. Vertex-to-vertex distance computation

In order to identify the relevant bone segments, the smallest distances between bone and obturator vertices are calculated. First, a vertex on the obturator surface is selected. Next, the Euclidian distance, or smallest distance between two points, from this single obturator vertex to every vertex on the skull surface is calculated. The smallest distance found is the smallest distance between that unique obturator vertex and the skull vertices. The distance value is stored as a label associated with the unique obturator vertex. This is repeated for every obturator vertex. This results in a smallest distance label for every obturator vertex to be added to a minimal distance map. A schematic version of this process with a limited amount of vertices can be seen in figure 14. The pseudocode that describes the steps to calculate the label for every obturator vertex can be seen on the right of figure 14.

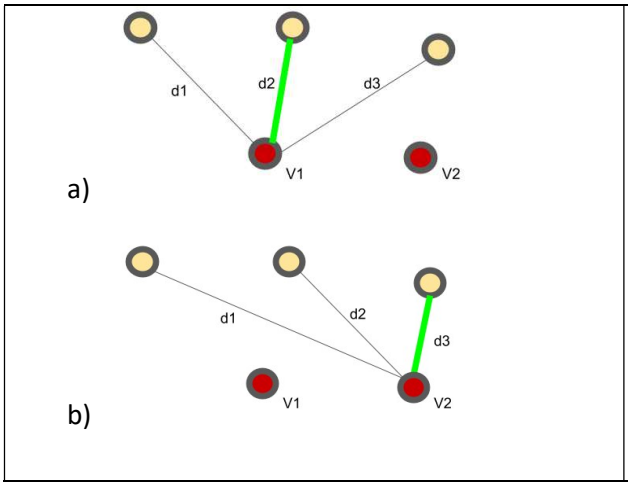


```
For i =  1: vertices in obturator
D_min = Inf
   For j = 1: vertices in skull
       V = obt_vertex(i) – skull_vertex(j)
       D_temp = sqrt(v*v')
                              If D_temp < D_min
          D_min = D_temp
          End
   End
D_label(i) = D_min
End
```

Figure 14: Two dimensional schematic representing the computation of the vertex-to-vertex distance (left), pseudocode(right)

(a) The distance of obturator vertex V1 to every yellow skull vertex is calculated. Green line D2 is the smallest distance. Therefore the label attributed to V1 has the value of d2.

(b) Next, the distance of obturator vertex V2 to every yellow skull vertex is calculated. In this case green line d3 is the smallest distance. Therefore the label attributed to V2 has the value of d3.

3.2.3. Grouping into clusters of vertices.

The focus lies on retrieving the smallest values in the distance label map as these represent the vertices with the closest relation to the skull mesh. Therefore, all vertices with distance label equal or smaller than three millimetre are selected. This produces a selection of vertices that we want to segment into several clusters. Matlab offers a function to group points in a point cloud. Therefore, the selected vertices are transformed to a point cloud. The native Matlab function '*pcsegdist*' identifies clusters of points that are close together and attributes an incremental number to each cluster of points. Points were attributed to different clusters if they were further apart than the minimal distance of 2 millimetres. This value was determined by trial-and-error, to be the best way to produce clusters that represented anatomical skull segments.

A schematic version of the way the clustering is performed is shown in figure 15.

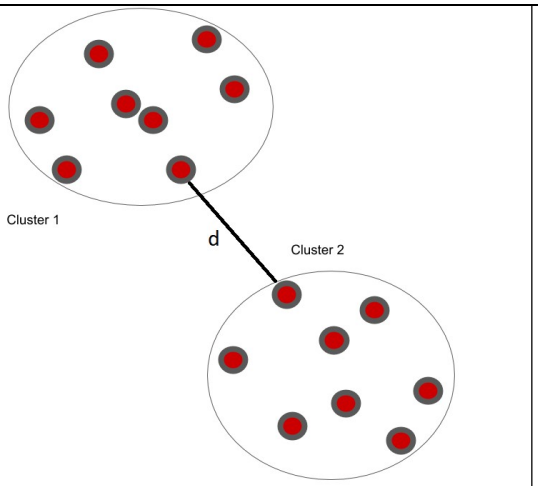


```
Int_verts = obt_vertex(D_label<=3)

ptCloud = pointCloud(int_verts)

[label, numClusters] = pcsegdist(ptCloud,2)
```

Figure 15: Two dimensional schematic representation of the grouping into clusters of vertices. Two groups of obturator vertices are more than d= 2mm apart. Therefore, they are attributed to separate clusters 1 and 2. (left), pseudocode (right)

3.2.4. From point cloud to faces and vertices.

In order to identify the bone segments that correspond to the clusters of obturator vertices, these clusters need to be visualised. Therefore we need to retrieve the faces that connect the vertices in each cluster. Every obturator face is selected that contains at least one vertex from the set of cluster vertices. The resulting selection of faces also contains faces that are connected to the outer edge of the cluster and only have one or two vertices from the cluster set. In order to exclude these outlier faces, the faces that are composed of three vertices represented in the set of cluster vertices are selected. A schematic version can be seen in figure 16.

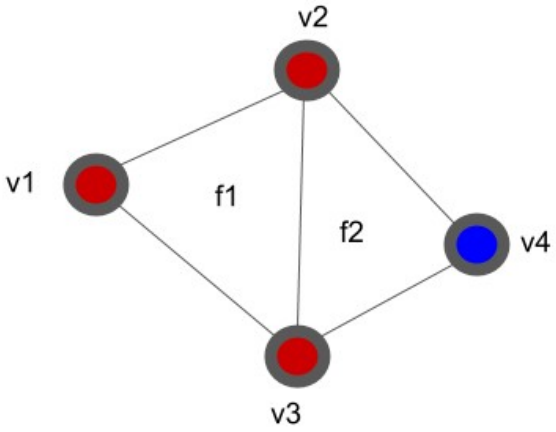


```
Int_faces = find(ismember(obt_face, int_verts)
FullVerts = obt_face(int_faces,:)
For i = 1:size(FullVerts,1)
   If FullVerts(i,1) is a member of int_verts and…
      FullVerts(i,2) is a member of int_verts and…
      FullVerts(i,3) is a member of int_verts

            faceFlag(i,1) = 1;
   End
End

IntervalFaces = Int_faces(faceFlag)
```

Figure 16: Schematic representation of the way faces are retrieved by evaluating the vertices it is composed of. The red vertices (v1-v2-v3) are part of a cluster. To retrieve the number of f1, the face list is evaluated for the appearance of faces containing v1, v2 or v3. This creates a shortlist of every face that is connected to the cluster vertices. However, f2 will also be selected. In order to only select f1, only faces that are composed of cluster vertices in all three positions are selected from the shortlist.

3.2.5. Visualisation

The clusters of obturator faces are visualised in red. All faces that were not included in the clusters because their distance to bone was too large are visualised in blue. This allows visual inspection of the clusters on the obturator surface. The skull may be visualised to aid in the correlation of clusters and their corresponding anatomical bone segments.

3.2.6. Computation of per cluster statistics.

In addition to identifying the bone segments that are in close relation to the obturator surface, the clusters can also be used to compute the statistics of all minimal distance labels of vertices in a cluster. For every cluster that identified to be a bone segment, the mean, median, standard deviation and minimal value are computed over all vertices in that cluster.

3.3. Results

3.3.1. Skull and obturator segmentation

The skulls and obturators were successfully segmented from the CTRT datasets and are visualised in figure 17.

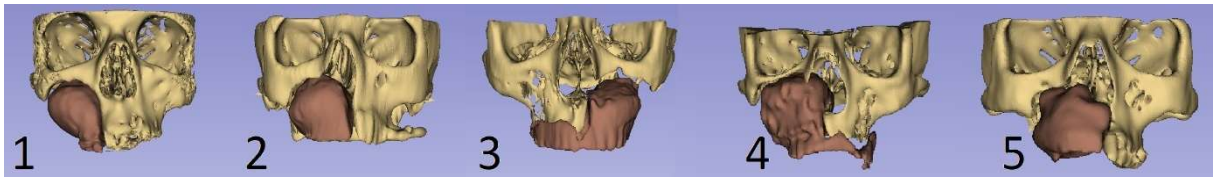

Figure 17: Segmentations of skull and obturator of five included patients. Patient 3 is seen to be edentulous and the defect is left sided. The other patients have remaining dentition and are right side defects. Patient 5 shows a Brown class II-d defect, whereas the other patients show class II-b defects.

3.3.2. Visualisation of clusters of obturator vertices on the obturator surface.

Visualisation of the clusters on the obturators resulted in the selection of five bone segments that showed recurrent close proximity to the obturator surface in multiple patients (figure 18) .

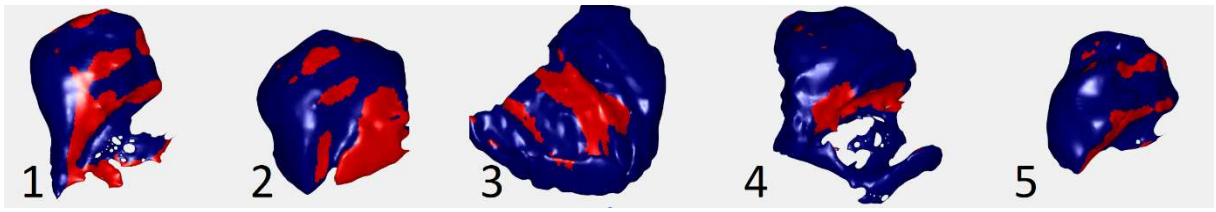

Figure 18: Clusters of close proximity between obturator and remaining bone of skull of five patients. The clusters of vertices with a small distance to a skull segments can be seen in red. The other obturator vertices, that are further away, are coloured blue. The numbers one thru five correspond to the patients in figure 17.

Five relevant anatomical bone segments were identified that have a recurring close proximity to the obturator. These segments are:

- Palatine resection margin
- Anterior wall of maxillary sinus
- Roof of maxillary sinus
- Vomer
- Pterygoid process.

3.3.3. Per cluster statistics.

The palatine resection margin has a smaller distance to the obturator surface than the other four bone segments (figure 19). Furthermore, the anterior wall of the maxillary sinus shows the largest distance of the five selected bone segments.

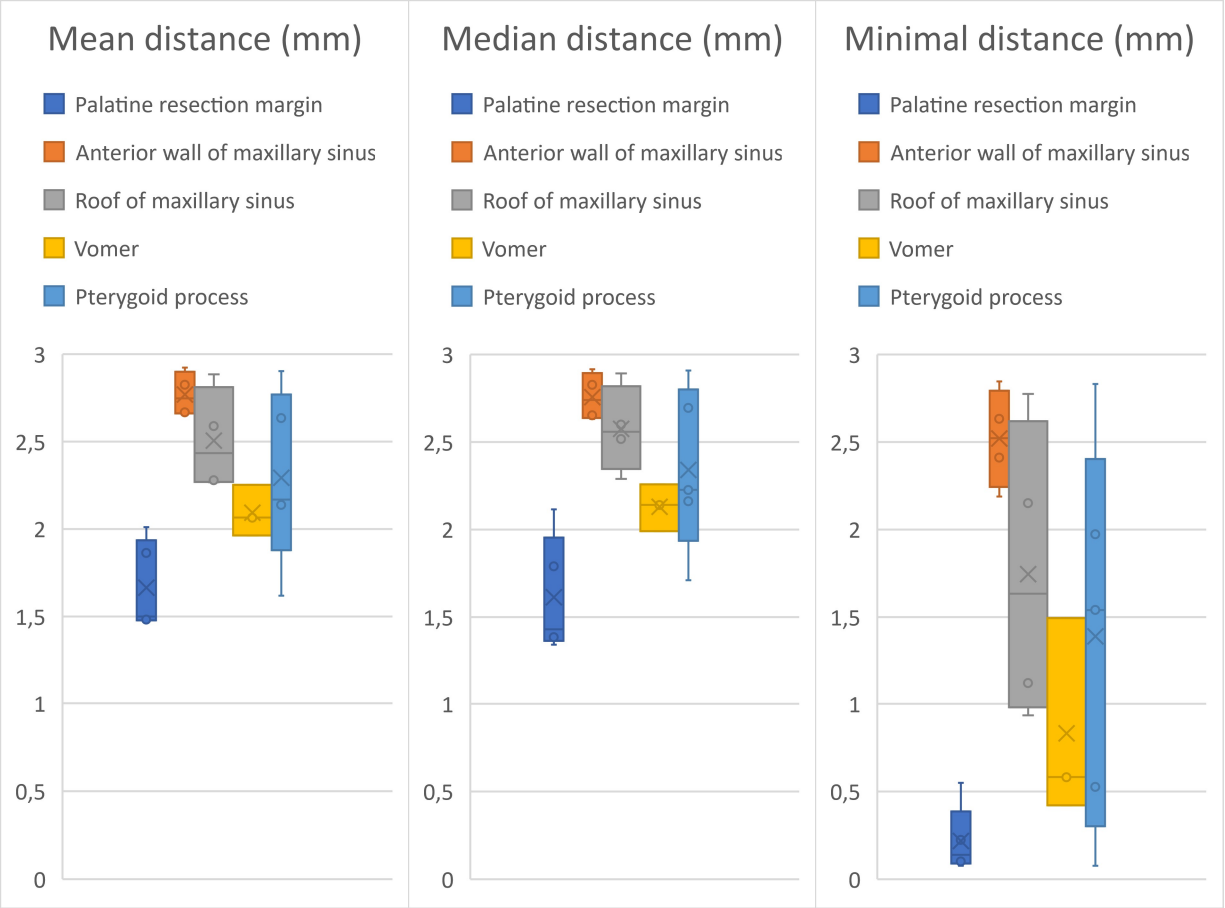

Figure 19 Mean, standard deviation and minimal distance to obturator surface of the five selected bone segments:

The mean distance and its standard deviation were calculated and can be seen in table 2.

Anatomical bone segment	Mean (mm)	SD (mm)
Palatine resection margin	1,67	0,71
Anterior wall of maxillary sinus	2,77	0,15
Roof of maxillary sinus	2,50	0,35
Vomer	2,06	0,58
Pterygoid process	2,29	0,44

Table 2: Bone segments with close relation to the obturator surface

3.4. Discussion

The results show that the palatine resection margin tends to have a close relation to the obturator. This is the area on the medial surface of the obturator where the baseplate transitions into the bulb. A close relation is desired in this location as this is where the seal that separates the oral and nasal cavities is maintained. The other four bone segments show a larger distance to the obturator surface. These segments are all located near the superior surface of the obturator. Therefore, the larger difference may be attributed to the effects of gravity that have pulled down the obturator from the bone.

The obturators that have been segmented in this study are intermediate obturators that have been in place for four to six weeks. This means that the soft tissue of these patients has started healing and that the tissue will now have started to compress due to the formation of scar tissue. In general, surgical obturators are larger than intermediate obturators due to the settling of tissue over time. This implies that a thicker layer of relining material will have to be applied to the proposed solid bulb to reach the size of the surgical obturator.

A big limitation is the fact that the intermediate obturators were not fixated to the patient during the scan. Therefore, it is possible that the superior bone regions are further from the obturator surface than would be the case in a fixated surgical obturator.

Table 2.2 shows the mean distance of the surfaces and its standard deviation. We assume that these five patients are representative for every class II-a or class II-d hemi-maxillectomy, and that the distance values follow a normal distribution. The combination of mean and three standard deviations provides a distance that will be exceeded in 0.135% of comparable cases. This results in a margin for bone segments of about four millimetres between the rigid dome and the bone segments. The palatine resection margin shows a minimal distance and mean that is much closer to the bone than four millimetres. Considering the anatomical location of this segment at the transition from baseplate to bulb, a margin of less than four millimetres is suggested for this bone segment.

It is important to note that these numbers are based on a very small subset of five patients that had a one-sided maxillectomy. Therefore, it is to be expected that these cases may not be fully representative for the whole population of class II-b and class II-d maxillectomy patients. Future research may aim to include other Brown classes, as the differences in anatomy suggest that the results may be completely different.

The distance between obturator surface and bone can never be smaller than zero. This results in a distribution of the distance values that does not follow a normal distribution but is skewed to the right. Skewing of the distribution results of a shift of the mean to a higher value. In this case that will result in the mean distance being overestimated. This is desirable as it results in a more robust margin. A small margin would allow larger dimensions of the bulb and consequently allow a larger air pocket. However, it would also result in an obturator that is more likely to impact bone segments when it is inserted into the surgical defect.

Low dose radiotherapy planning scans have been used in this study. A high resolution CT scan would increase the quality of the bone and obturator segmentations. However, the associated high radiation dose associated with this type of scan cannot be justified from an ethical point of view. One could say that radiotherapy causes a larger dose than an supplementary CT scan. However, the dose administered during radiotherapy is therapeutic, while the dose administered in a study related CT

scan is not. An additional scan may be a threat to the patient without providing a direct benefit to the patient.

The five bone areas that have been identified in chapter three, do not fully describe the optimal shape of the bulb. However, they provide limits that can guide the dimensions at specific locations at the obturator surface. Areas that have a close relation to soft tissue but not to bone, such as the tissue of the cheek, or that are exposed to air, such as the nasal cavity, have not been taken into account in this study. Initially, these areas will have to be extended using a thicker application of the outer relining material to achieve the proper amount of extension. Further research should focus on expanding the dataset with other Brown class patients, to evaluate whether the four millimetre margin can be generalised to other types of maxillectomy.

The five bone areas may serve as the first step towards the bone guided design of the bulb. A very basic way to achieve this is to link the five bone areas together. This provides the outer margins of the obturator. A successive step could be to extend this using region growing to close the area in between. A further complication of such an automated design application could be to use the vertex-to-vertex distance map to guide the shape of the obturators surface in relation to bone segments. This model would greatly benefit from the expansion of the database with obturator models of the same Brown class, as this may lead to an 'average obturator' that can be used as a base model that will be adjusted based on the specific tumour and anatomy of the patient.

Implementation of CT and MR based traditional baseplate planning would also greatly benefit the digital design of obturators. This is expected to produce a more accurate way of predicting the tumour resection margins. This could be further verified if a per-surgical or post- surgical scan were to be added to the current workflow. A recent publication showed that intraoperative evaluation of resection margins using CBCT imaging is a promising way to assess the resection defect and indicate compliance with the intended resection[26].

More insight into the actual relation of the surgical obturator surface to the bony resection margins is relevant for the future verification of the bulb design. The use of electromagnetic(EM) navigation equipment provides opportunities to compare the surgical defect to the intended resections. Unpublished work shows that intraoperative evaluation of resection margins appears to be very promising. This offers the surgeon a tool to evaluate whether the intended resection planning has been executed successfully and clean resection margins are to be expected. The EM system can also be utilised for the intraoperative verification of the five bony segments as proposed in this chapter. This is required to validate the four millimetre distance margin that was proposed and evaluate whether a smaller margin should indeed be taken into account for the palatine resection margin.

3.5. Conclusion

The study described in this chapter has resulted into the identification of five bone areas that were in close proximity to the obturator surface. These are the palatine resection margin, which had the closest relation to bone, and the anterior wall of the maxillary sinus, the roof of the maxillary sinus, the vomer and the pterygoid process, which showed a slightly larger distance.

The acceptable closest obturator bulb distance to these bony structures of four millimetres is suggested. The results show that this distance is likely to be smaller for the palatine resection margin bone as there is a need for close contact to provide sealing between oral and nasal cavities.

4. From a baseplate design and a bulb design to the digital design of an obturator

In chapter two, the digital design workflow for a baseplate has been proposed. This workflow has been used to design a digital designed baseplate that showed no large variation from the traditional design baseplate. After 3D printing of the digitally designed baseplate, it was successfully tested in vivo. In chapter three, five bone areas have been identified that showed a close relation to the obturator surface. Furthermore, a bone to obturator surface margin of 4 mm has been proposed as a conservative estimate of the distance that should be taken into account in a digital design printed obturator.

These two chapters and their results provide the very first steps towards the full implementation of the digital design of a workflow. However, the implementation of such a digital design workflow still requires a lot of work. This chapter focusses on the combination of the rigid obturator bulb and the baseplate to come to a one-piece obturator and how these two first steps may lead to further development towards a digital design workflow.

The first step onwards is the combination of the digital baseplate and the digital bulb into a full digital design for an obturator. This may be achieved in the near future as fusion of the bulb and the baseplate can be achieved digitally to form a one piece obturator. At this stage, an air pocket can also be added to the bulb to achieve weight reduction. Weight reduction of the obturator is essential in order to increase patient comfort.

The current bulb margin was calculated based on a set of 5 intermediate obturators instead of surgical obturators. These obturators have been modified in the weeks after surgery to accommodate wound healing and optimise patient comfort. In general, intermediate obturators are smaller than surgical obturators due to the removal of material in this process. This results in underestimation of the size of the surgical obturator in this study and overestimation of the required relining material thickness. This will result in the application of a thicker relining layer to expand the bulb to the dimensions required for a surgical obturator bulb. However, in the long term this can possibly be beneficial. Currently, an intermediate obturator is produced several weeks after surgery that is smaller in size than the surgical obturator. This may become obsolete when the intermediate obturator can be already incapsulated into the digitally designed surgical obturator. In that case, the relining material can easily be trimmed down using a surgical knife when adaptation of the obturator shape is required.

Currently, the target is formulated that the time between the first time the patient is seen by a medical professional up to start of therapy should not exceed 30 days. The digital design of the obturator may accelerate the way obturators are made. The digital workflow does eliminates several repetitions of the time consuming casting and curing process used to produce the current baseplate. In addition, the digital design can be altered at any time and previous steps can be reloaded once a design choice appeared suboptimal. During the digital design process, the accurate fit of the baseplate can be verified at any time as the digital dental model is available.

The digital nature of the design workflow facilitates faster multidisciplinary communication. The different imaging modalities like CT, MR, and intraoral scanner can be combined in one patient specific model. This model can be expanded with tumour delineations, intended resection margins, consequent cutting planes, dental elements to be extracted and intended locations for implant placement or other ways of fixation. Next, the model will serve as a starting point for digital obturator design.

5. Clinical implementation and future perspectives

The previous chapters have shown how digital design of an obturator is feasible. However, the full implementation in the current clinical workflow is still far away. This is primarily caused by the large amount of steps in the current workflow that need to be adapted to a digital form. Each step takes time and effort to be modified which makes implementation of at once a challenging operation , the separation of the workflow in multiple steps also provides opportunities for modular implementation of parts of the digital workflow. Several steps can be identified that together provide a structure for a future digital workflow.

Data-acquisition

High quality CT, MR, and IOS data are merged into a 3D patient model. Currently, this data is not available which may prevent the successful delineation of tumour and resection margins. These availability of accurate margins is essential for the accurate digital design of an obturator.

Surgical planning

The imaging and combination of CT/MR/IOS and delineation into a 3D patient model provide the surgical team with a way of accurately visualising and documenting the tumour and the intended resection margin. In addition, the maxillofacial prosthetist can add information concerning the oral state and preferred ways of obturator fixation. This leads to a *pre-surgical status and planning model* that can be discussed during the presurgical reconstruction meeting.

Image guided surgery

The actual surgical resection margin can be compared to the intended resection margin. This provides insight into the possible fit and also provides imaging data that can be used in the design of the intermediate obturator. The implementation of electro magnetic navigation is expected to provide the surgeon with an intraoperative way of verifying the resection margin. This is essential as a digitally designed obturator will show optimal fit when the planned defect and the surgical defect are comparable.

Design

The design of the obturator strongly benefits from the availability of a traditional baseplate patient model. In this model the intended resection margin provides an indication of the location of bone cuts. This can be used to design the digital baseplate and the bulb. This study shows that the bulb surface is close to the palatine resection margin. A distance of four millimetres is suggested for the four other bone segments evaluated in this study.

Additive manufacturing

The digital design of the obturator provides a model that can be produced using additive manufacturing. Additive manufacturing allows the addition of a hollow space to the obturator bulb which reduces obturator weight.

Relining

The obturator will require a relining layer to achieve a good fit in the patient (figure 6). The liner provides increased contact area between the rigid bulb and the soft tissue. It may be applied during surgery and be modified as changes in the tissue arise.

Digitalization

Once the surgical obturator is finished, it can be digitized by scanning it using CT, structured light scanning or IOS imaging. This is performed prior to the fixation into the patient. This provides the possibility to identify the actual thickness of the relining material. This model can also be used as feedback to improve the digital design stage. Most importantly, it provides information about the shape and size of the defect that can be used to prepare the design and manufacturing of the intermediate obturator.

Once implemented, the above workflow provides a way of producing an obturator that is lower in weight and may require the patient to return to hospital less often. Furthermore, digital design also promotes the creation of a database with every previous design. This may lead to a classification of different classes of obturators for different classes of maxillectomy defects. A digital database of obturators is also beneficial for the patient. In case their current obturator is damaged, a new version can be printed and delivered on short notice.

This shows that a lot of work has to be done before digital design is implemented. It also shows that the implementation of digital design and additive manufacturing of the obturator is currently limited by the accuracy of the defect prediction and by the lack of experience with digital design and printing. However, this should not be a reason to postpone the implementation of digital design. In the end, it takes a long time to implement, and transition to, a full digital workflow. Therefore, one should start early.

5.1. A proposed semi-digital workflow

The following modified workflow is proposed as a way to start gaining experience with digital design and additive manufacturing of the obturator and improve patient comfort. At all times it allows conversion to the traditional obturator workflow.

1. The obturator is designed and produced in the traditional way however an intraoral scan is made during the first visit.
2. The digital baseplate is designed parallel to the traditional plate.
3. The traditional baseplate is scanned to acquire a digital version.
4. The digital baseplate is compared to the traditional baseplate.
5. The traditional obturator is produced using the traditional baseplate and putty bulb
6. Prior to fixation, the traditional obturator with putty bulb is scanned using the intraoral scanner and/or CBCT.
7. The patient receives the traditional obturator.
8. During the two weeks between surgery and the first removal of the traditional obturator, the intermediate obturator is designed digitally, based on the digital version of the baseplate and the digital version of the surgical obturator. A hollow bulb is added.
9. The intermediate obturator is printed.
10. The digital version of the traditional surgical obturator may guide the application of relining material to the intermediate obturator.
11. The hollow intermediate obturator can be placed when the fixated surgical obturator is removed two weeks after surgery.
12. Remodelling of the relining material can be performed on the spot, the patient is awake and can provide feedback.

Several advantages can be identified from this semi-digital design approach.

- The production of the intermediate obturator is not delayed by the two week waiting period until the surgical obturator can be duplicated.
- The intermediate obturator can be placed when the surgical obturator is first removed after two weeks.
- The scanning of the traditional surgical obturator during surgery provides a high quality model of the obturator. But also a high quality representation of the resection defect. This promotes the optimal design of the rigid bulb and maximization of the air pocket. Consequently, it reduces the need for a thick layer of relining material.

This proposed workflow has been visualised in figure 20 as a modification to the current workflow that was presented in chapter one.

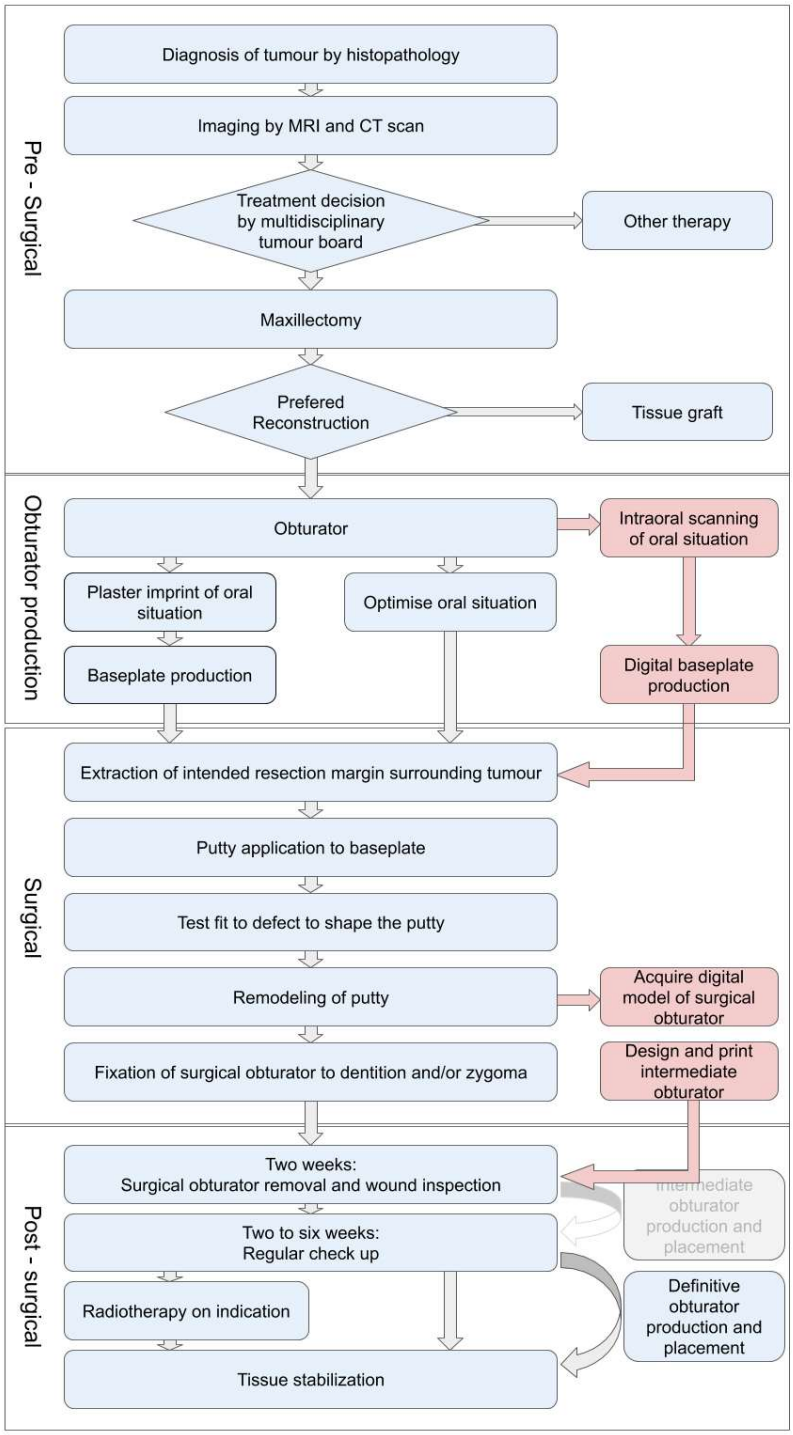

Figure 20: proposed modified workflow (in red) that offers parallel implementation of digital workflow in intermediate obturator production. The use of the intraoral scanner provides a model that can be used to digitally design and produce a baseplate. This can be performed in parallel to the traditional baseplate production and leads to an increase in experience and provides data that can be used to further improve the workflow. The second modification targets the intermediate obturator. This can again be performed in parallel to the traditional workflow. A digital model of the surgical obturator is acquired per-surgically. This model can be used to produce a hollow intermediate obturator that can be placed two weeks after surgery, when the surgical obturator is first removed.

6. General conclusion

The design of the current surgical obturator is not based on traditional baseplate delineation of the tumour and associated resection margins in CT and/or MR. This results in limited prior insight into the shape and extend of the defect that will be created during the maxillectomy procedure and prevents the presurgical production of a hollow surgical obturator. The surgical obturator is based on the intraoperative combination of a premade baseplate, which covers the defect, and a putty bulb, which fills the defect. The putty bulb is heavy which results in reduced patient comfort.

This study showed that the digital design of a surgical baseplate is possible and that the production of an identical baseplate is possible if clear design criteria are defined. A margin of four millimetre has been proposed for the distance between five bone segments in the defect region and the obturator surface in Brown class II-a and II-d defects. However, these results need verification both by the acquisition of high quality imaging data and by increasing the number of cases that are evaluated.

The introduction of a digital workflow offers new ways of designing and producing obturators. That are expected to provide reduced production time, reduced surgical time and increased patient comfort. However, it also shows the need for the introduction of digital delineation in the presurgical planning stage and illustrates the need for verification of results during and after surgery.

The first steps to start introduction of digital design into the current workflow have condensed into the proposal for a semi-digital workflow. This aims increase the collective experience of the team with digital design and is expected to provide many opportunities for further research.

7. List of References

[1] Nederlandse Werkgroep Hoofd-Halstumoren, “Richtlijn mondholte-en orofarynxcarcinoom.” Alphen aan den Rijn: Van Zuiden Communications B.V., 2004.

[2] J. Breeze *et al.*, “Health-related quality of life after maxillectomy: obturator rehabilitation compared with flap reconstruction,” *Br. J. Oral Maxillofac. Surg.*, vol. 54, no. 8, pp. 857–862, Oct. 2016.

[3] G. Michelinakis, M. Pavlakis, and D. Igoumenakis, “Rehabilitation of a maxillectomy patient using intraoral scanning impression technology and a computer-aided design/computer-aided manufacturing fabricated obturator prosthesis: A clinical report.,” *J. Indian Prosthodont. Soc.*, vol. 18, no. 3, pp. 282–287, 2018.

[4] M. A. Pogrel, “Inferior hemi-maxillectomy for treatment of palatal tumors,” *J. Oral Maxillofac. Surg.*, vol. 46, no. 1, pp. 85–87, Jan. 1988.

[5] T. Mücke, D. J. Loeffelbein, B. Hohlweg-Majert, M. R. Kesting, K.-D. Wolff, and F. Hölzle, “Reconstruction of the maxilla and midface – Surgical management, outcome, and prognostic factors,” *Oral Oncol.*, vol. 45, pp. 1073–1078, 2009.

[6] A. Eskander, S. Y. Kang, T. N. Teknos, and M. O. Old, “Advances in midface reconstruction: Beyond the reconstructive ladder,” *Current Opinion in Otolaryngology and Head and Neck Surgery*, vol. 25, no. 5. pp. 422–430, 2017.

[7] J. S. Brown and R. J. Shaw, “Reconstruction of the maxilla and midface: introducing a new classification,” *Lancet Oncol.*, vol. 11, pp. 1001–1008, 2010.

[8] S. Iyer and K. Thankappan, “Maxillary reconstruction: Current concepts and controversies.,” *Indian J. Plast. Surg.*, vol. 47, no. 1, pp. 8–19, Jan. 2014.

[9] G. S., D. K.P., and B. G., “Prospective study to evaluate quality of life and improvement in speech with and without maxillary prosthesis in patients with maxilectomy,” *Support. Care Cancer*, vol. 19, no. 2, p. S182, 2011.

[10] M. Singh, A. Bhushan, S. Chand, and N. Kumar, “Obturator prosthesis for hemimaxillectomy patients,” *Natl. J. Maxillofac. Surg.*, vol. 4, no. 1, p. 117, 2013.

[11] H. Shengwei, W. Zhiyong, H. Qingang, and H. Wei, “Combined Use of an Anterolateral Thigh Flap and Rapid Prototype Modeling to Reconstruct Maxillary Oncologic Resections and Midface Defects,” *J. Craniofac. Surg.*, vol. 25, no. 4, pp. 1147–1149, Jul. 2014.

[12] Y. Y. Wang, S. Fan, H. Q. Zhang, Z. Y. Lin, J. T. Ye, and J. S. Li, “Virtual surgical planning in precise maxillary reconstruction with vascularized fibular graft after tumor ablation,” *J. Oral Maxillofac. Surg.*, vol. 74, no. 6, pp. 1255–1264, 2016.

[13] T. Jiao, C. Zhu, X. Dong, and X. Gu, “Rehabilitation of Maxillectomy Defects with Obturator Prostheses Fabricated Using Computer-Aided Design and Rapid Prototyping: A Pilot Study,” *Int. J. Prosthodont.*, vol. 27, no. 5, pp. 480–486, 2014.

[14] G. Tirelli *et al.*, “Obturator prostheses following palatal resection: clinical cases.,” *Acta Otorhinolaryngol. Ital.*, vol. 30, no. 1, pp. 33–9, Feb. 2010.

[15] G. J. Paprocki, “Maxillofacial prosthetics: history to modern applications. Part 1 - obturators.,” *Compend. Contin. Educ. Dent.*, vol. 34, no. 8, pp. e84-6, Sep. 2013.

[16] A. Farias, C. Hegde, and D. Krishnaprasad, “A simplified technique to make an immediate

surgical obturator for a maxillectomy patient," *J. Interdiscip. Dent.*, vol. 3, no. 2, p. 125, 2013.

[17] J. Kortes, H. Dehnad, A. N. T. Kotte, W. M. M. Fennis, and A. J. W. P. Rosenberg, "A novel digital workflow to manufacture personalized three-dimensional-printed hollow surgical obturators after maxillectomy," *Int. J. Oral Maxillofac. Surg.*, 2018.

[18] F. Banu Raza, M. Choudhary, A. Kumar, A. Inbarajan, M. Kumar, and P. Natarajan, "Surgical to Interim–Chairside Management of Hemimaxillectomy Patient," *Otolaryngology*, vol. 07, no. 01, pp. 1–2, Feb. 2017.

[19] R. J. Murphy, C. R. Gordon, E. Basafa, P. Liacouras, G. T. Grant, and M. Armand, "Computer-assisted, Le Fort-based, face–jaw–teeth transplantation: a pilot study on system feasiblity and translational assessment," *Int. J. Comput. Assist. Radiol. Surg.*, vol. 10, no. 7, pp. 1117–1126, Jul. 2015.

[20] K. Torabi, E. Farjood, and S. Hamedani, "Rapid Prototyping Technologies and their Applications in Prosthodontics, a Review of Literature," *J Dent Shiraz Univ Med Sci. J Dent Shiraz Univ Med Sci*, vol. 16, no. 161, pp. 1–9, 2015.

[21] P. Tack, J. Victor, P. Gemmel, and L. Annemans, "3D-printing techniques in a medical setting: a systematic literature review.," *Biomed. Eng. Online*, vol. 15, no. 1, p. 115, Oct. 2016.

[22] E. T. W. Tan, J. M. Ling, and S. K. Dinesh, "The feasibility of producing patient-specific acrylic cranioplasty implants with a low-cost 3D printer," *J. Neurosurg.*, vol. 124, no. 5, pp. 1531–1537, May 2016.

[23] A. Aldaadaa, N. Owji, and J. Knowles, "Three-dimensional Printing in Maxillofacial Surgery: Hype versus Reality," *J. Tissue Eng.*, vol. 9, pp. 1–5, 2018.

[24] J. M. Plooij, T. J. J. Maal, P. Haers, W. A. Borstlap, A. M. Kuijpers-Jagtman, and S. J. Bergé, "Digital three-dimensional image fusion processes for planning and evaluating orthodontics and orthognathic surgery. A systematic review," *Int. J. Oral Maxillofac. Surg.*, vol. 40, no. 4, pp. 341–352, Apr. 2011.

[25] L.-E. Rännar and J.-M. Hirsch, "Imaging, Virtual Planning, Design, and Production of Patient-Specific Implants and Clinical Validation in Craniomaxillofacial Surgery," *Craniomaxillofac Trauma Reconstr.*, vol. 5, pp. 137–144, 2012.

[26] O. Ivashchenko *et al.*, "Intraoperative verification of resection margins of maxillary malignancies by cone-beam computed tomography.," *Br. J. Oral Maxillofac. Surg.*, vol. 57, no. 2, pp. 174–181, Feb. 2019.

[27] M. Braden, P. S. Wright, and S. Parker, "Soft lining materials--a review.," *Eur. J. Prosthodont. Restor. Dent.*, vol. 3, no. 4, pp. 163–74, Jun. 1995.

[28] M. M. Mutluay and I. E. Ruyter, "Evaluation of bond strength of soft relining materials to denture base polymers," *Dent. Mater.*, vol. 23, no. 11, pp. 1373–1381, Nov. 2007.

[29] C. L. Bohle III, G. C., Estilo and J. M. Huryn, "Figure 38.2," in *Grabb and Smith's Plastic Surgery*, 7th ed., .

[30] A. Dawood, B. M. Marti, V. Sauret-Jackson, and A. Darwood, "3D printing in dentistry," *Br. Dent. J.*, vol. 219, no. 11, pp. 521–529, 2015.

[31] O. S. Gursharan Kaur Sason, Gaurang Mistry, Rubina Tabassum, "A comparative evaluation of intraoral and extraoral digital impressions: An in vivo study," *J. Indian Prosthodont. Soc.*, vol. 17, no. 4, pp. 406–411, 2018.

[32] A. O. Ali, “Accuracy of Digital Impressions Achieved from Five Different Digital Impression Systems,” *Dent. Ali, Dent.*, vol. 5, no. 5, 2015.

[33] H.-N. Park, Y.-J. Lim, W.-J. Yi, J.-S. Han, and S.-P. Lee, “A comparison of the accuracy of intraoral scanners using an intraoral environment simulator.,” *J. Adv. Prosthodont.*, vol. 10, no. 1, pp. 58–64, Feb. 2018.

[34] R. Nedelcu, P. Olsson, I. Nyström, J. Rydén, and A. Thor, “Accuracy and precision of 3 intraoral scanners and accuracy of conventional impressions: A novel in vivo analysis method,” *J. Dent.*, vol. 69, pp. 110–118, Feb. 2018.

[35] S. Klein, M. Staring, K. Murphy, M. A. Viergever, and J. Pluim, “elastix: A Toolbox for Intensity-Based Medical Image Registration,” *IEEE Trans. Med. Imaging*, vol. 29, no. 1, pp. 196–205, Jan. 2010.

[36] R. Kikinis, S. D. Pieper, and K. G. Vosburgh, “3D Slicer: A Platform for Subject-Specific Image Analysis, Visualization, and Clinical Support,” in *Intraoperative Imaging and Image-Guided Therapy*, New York, NY: Springer New York, 2014, pp. 277–289.

[37] S. Rusinkiewicz and M. Levoy, “Efficient Variants of the ICP Algorithm.”

[38] Autodesk, “Meshmixer.” Autodesk, San Rafael, CA, USA, 2017.

[39] “Matlab (2018b).” The MathWorks Inc., Natick, Massachusetts, 2018.

[40] H. Gray, W. H. (Warren H. Lewis, and I. Bartleby.com, *Anatomy of the human body*. Bartleby.com, 2000.